Natural analogues of planet Mercury's surface: Mineralogical and spectroscopic aspects

Anna Irene Landi
Department of Phisics, University of Trento, Via Sommarive 14, 38123 Trento
Department of Earth Sciences, University of Firenze, Via G. La Pira 4, 50121 Firenze

DOI: 10.19276/plinius.2026.01.008

INTRODUCTION

Understanding the nature and evolution of Mercury's surface materials is crucial to constrain the planet's formation processes. Studying the processes that led to the formation of Mercury is essential to understanding the formation and evolution of rocky planets (*e.g.*, Solomon et al., 2018). Data from NASA's MESSENGER (MErcury Surface, Space ENvironment, GEochemistry, and Ranging) mission indicate that the surface is dominated by Na-rich plagioclase, FeO-poor enstatite and forsterite, and Mg–Ca–Fe sulfides, suggesting that Mercury formed in the inner part of the protoplanetary disk from highly reduced precursor materials (*e.g.*, Nittler & Weider, 2019). However, the interpretation of Mercury's spectral properties remains complex due to the effects of space weathering (SpWe) and extreme temperature variations affecting the surface (*e.g.*, Domingue et al., 2014; Maturilli et al., 2014). Since direct information on the surface is not available from Mercury meteorites or returned samples, the study of analogous materials is crucial for interpreting the upcoming data from the ongoing ESA-JAXA BepiColombo mission (Rothery et al., 2020).

I conducted a comprehensive minero-petrological and spectroscopic investigation on natural materials proposed as potential analogues of Mercury's surface, specifically highly reduced meteorites (Burbine et al., 2002; Udry et al., 2019; Wilbur et al., 2022) and terrestrial boninites (Vander Kaaden et al., 2017). In particular, aubrites, a rare group of highly reduced achondrites characterized by a heavily brecciated texture (Keil et al., 2010), have been proposed as a promising spectral analogue for Mercury's surface (Burbine et al., 2002), while terrestrial boninites have been proposed as analogues of the various Mercury's geochemical terranes (Weider et al., 2015), considering their bulk composition (Vander Kaaden et al., 2017). The investigated meteorites include five aubrites (Rantila, Tiglit, Peña Blanca Spring, Norton County, NWA 14185) and four enstatite chondrites, achondrites and melt rocks (EH7-an Itqiy, EL6 NWA 4945, enstatite achondrite NWA 13266, enstatite melt-rock NWA 13210). The terrestrial boninites come from three different localities of the Troodos Massif, Cyprus.

The mineralogical and compositional properties of these materials have been compared with their reflectance spectroscopy behaviour in the visible and near-infrared (VNIR) range and in the mid-infrared (MIR) range. In the spectral characterization of these materials the effects of Space Weathering (SpWe) and extreme temperature variations were taken into account through laboratory simulations.

By integrating mineralogical, chemical, and spectroscopic data from natural analogues of Mercury's surface, we can better constrain how composition, reduction state, and SpWe can influence spectral properties, highlighting the value of a multi-methodological approach. Moreover, this study provides a detailed spectral library of analogues that could help in the interpretation of Mercury's surface spectra from BepiColombo SIMBIO-SYS (Spectrometer and Imagers for MPO BepiColombo Integrated Observatory SYStem, Cremonese et al., 2020) and MERTIS (MErcury Radiometer and Thermal Infrared Spectrometer, Hiesinger et al., 2020) instruments, and in linking these spectra to the compositional data from MIXS (Mercury Imaging X-ray Spectrometer) instrument (Fraser et al., 2010).

METHODS

Scanning electron microscope (SEM) analyses were conducted at the Centro di Servizi di Microscopia Elettronica e Microanalisi (MEMA) laboratory of the Università degli Studi di Firenze for the investigation of texture and mineralogy. Backscattered electron (BSE) and energy-dispersive spectroscopy (EDS) maps were collected. Quantitative analyses of the detected mineral phases were performed at the Laboratorio di MicroAnalisi (LaMA) laboratory, Dipartimento di Scienze della Terra of the Università degli Studi di Firenze, through Electron Microprobe analyses (EPMA).

Reflectance spectra on polished slab, rock fragments and powdered samples were measured in the visible/near-infrared (VNIR) range and in the mid-infrared (MIR) range at the S.LAB. laboratory of INAF (Istituto Nazionale di Astrofisica) – IAPS (Institute for Space Astrophys-

ics and Planetology), Rome, and at the Planetary Spectroscopy Laboratory (PSL) of the German Aerospace Center (DLR), Berlin.

Ion irradiation experiments on aubrites, simulating solar wind irradiation on highly reduced object such as Mercury's surface, have been performed at the ING-MAR (IrradiatioN de Glaces et Météorites Analysées par Réflectance VIS-IR, IAS & IJCLab, Université Paris-Saclay, Orsay, France) facility using the SIDONIE electromagnetic isotope separator (Chauvin et al., 2004). Aubrites in form of both pellets and rock fragments have been irradiated with He^+ (20 keV) and C^+ (30 keV), with increasing fluence up to $1x10^{17}$ ions/cm^2. The spectral effects due to ion implantation have been investigated in situ after each irradiation step in the VNIR range, and ex-situ before and after the irradiation in the MIR range.

Boninites bulk composition has been determined through X-ray fluorescence (XRF) measurements at the *Centro di Servizi di Cristallografia Strutturale* (CRIST), *Università degli Studi di Firenze*. Their emissivity behaviour has been investigated using the emissivity chamber at PSL (Maturilli et al., 2017). The emissivity spectra in the MIR range were collected at 150°C, 250°C, 350°C, and 450°C. A black body sample (graphite) has been measured with the same procedure, and used for the data calibration (Ferrari et al., 2014).

RESULTS

Highly reduced meteorites

The investigated meteorites are mainly composed of nearly FeO-free enstatite. Aubrites present the typical brecciated texture and, following the predominant enstatite, they are composed of variable amounts of forsterite and diopside, minor Na-rich plagioclase, sulfides, and metals (Fig. 1a). Enstatite chondrites and achondrites lack olivine and clinopyroxene (with the exception of the EL NWA 4945), present higher amounts of plagioclase, and are enriched in metals and sulfides compared to aubrites (Fig. 1b). Glass and melt portion could be observed in all meteorite types, indicating that many of them may have undergone extensive or local melting processes.

The very low amount of FeO in silicates and the presence of exotic sulfides of Ca, Mg, Mn are indicative of highly reducing conditions. Silicates composition is similar among meteorites from different groups while sulfides and metals present higher variability. Enstatite average composition in aubrites is $En_{98.8}Wo_{0.7}Fs_{0.5}$ in Rantila, $En_{99.6}Wo_{0.3}Fs_{0.1}$ in Norton County, $En_{99.0}Wo_{0.9}Fs_{0.1}$ in Tiglit, and NWA14185; in enstatite chondrites and achondrites $En_{96.9}Wo_{3.0}Fs_{0.1}$ in Itqiy, $En_{98.3}Wo_{1.4}Fs_{0.3}$ in NWA 4945, $En_{99.0}Wo_{0.9}Fs_{0.1}$ in NWA 13266, $En_{98.4}Wo_{1.5}Fs_{0.1}$ in NWA 13210. Forsterite average composition in aubrites is $Fo_{99.7}$ in Rantila and $Fo_{99.9}$ in Norton County and Tiglit. Diopside average composition in aubrites

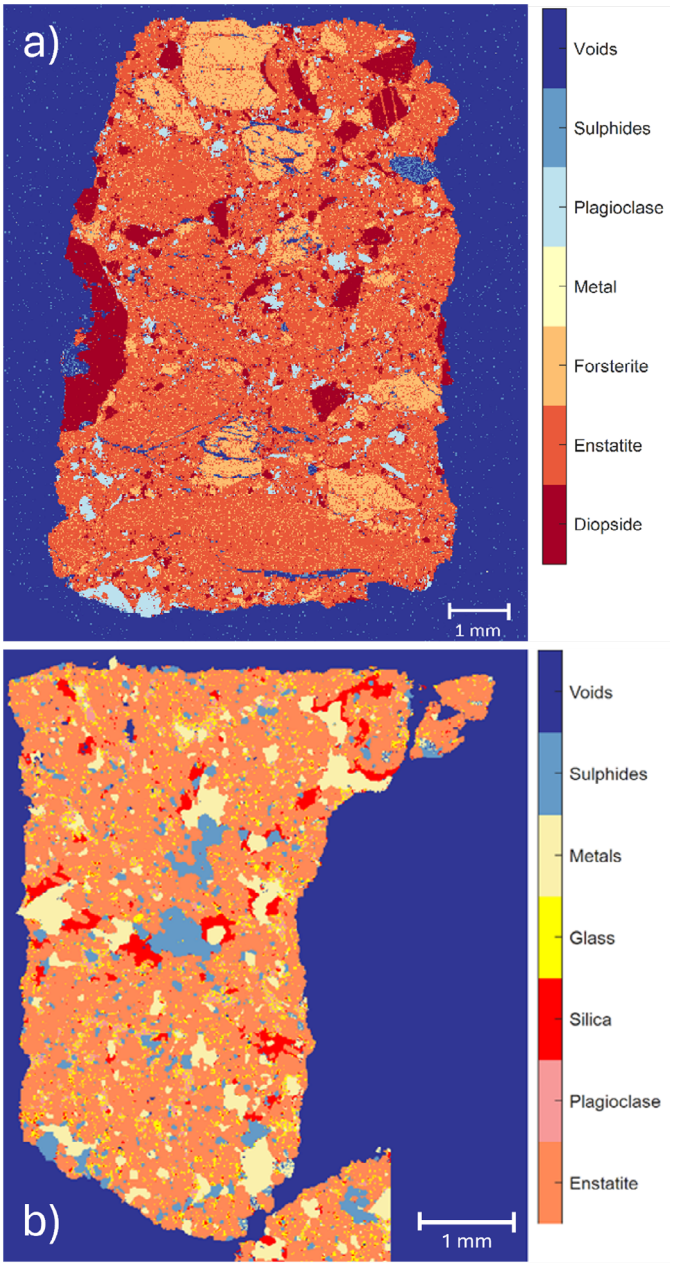

Figure 1 *EDS maps showing examples of the mineral assemblages found in the investigated meteorites.* ***a)*** *Rantila aubrite;* ***b)*** *NWA 13266 enstatite achondrite.*

is $En_{56.2}Wo_{43.6}Fs_{0.2}$ in Rantila, $En_{55.2}Wo_{44.6}Fs_{0.2}$ in Norton County, $En_{56.0}Wo_{43.9}Fs_{0.1}$ in Tiglit, and $En_{53.7}Wo_{46.2}Fs_{0.1}$ in NWA 14185; and $En_{53.7}Wo_{46.2}Fs_{0.1}$ in the enstatite chondrite NWA 4945. Plagioclase presents a wide range of chemical compositions in Rantila ($Ab_{79.5-95.6}Or_{1.5-10.0}An_{0.2-18.6}$) and Norton County ($Ab_{69.3-95.2}Or_{0.7-4.1}An_{0.7-30.0}$) aubrites, while in Tiglit aubrite it is mostly albitic and less variable ($Ab_{89.6-95.8}Or_{3.8-4.9}An_{0.1-6.2}$). Plagioclase composition within the enstatite chondrites and achondrites samples is homogeneous: $Ab_{81.9}Or_{4.9}An_{13.2}$ in NWA 4945, $Ab_{82.3}Or_{2.5}An_{15.2}$ in NWA 13266, $Ab_{79.7}Or_{4.2}An_{16.1}$ in NWA 13210. Ni concentrations in metals are, on average, higher in enstatite chondrites and achondrites than in aubrites. Si contents in metals are under EPMA detection limits or in little amounts (0.1–0.2 wt.%) in aubrites, around 0.4 wt.% in the enstatite achondrite NWA 13266, and one order of magnitude higher, around 2–3 wt.%, in enstatite chondrites. Troilite is the most abundant sulfide, present in all the investigated meteorite groups,

often associated to metals and daubréelite. Troilite most variable minor elements among the different samples are Cr and Ti: Cr amounts range from 0.4 to 4.1 wt.% in aubrites and from 2.7 to 5.1 wt.% in enstatite chondrites and achondrites; Ti amounts range from below detection limit to 3 wt.% for aubrites and from 0.4 to 2.2. wt.% for enstatite chondrites and achondrites. Fe, Mn, Mg, Ca sulfides present a wide range of chemical compositions: Mg-rich sulfides (Mg up to 15 wt.%) are present only in the enstatite achondrite NWA 13266; Fe-dominant sulfides (Fe up to 37 wt.%) are observed in enstatite chondrites and achondrites but not in aubrite; Mn-rich sulfides show Mn up to 49 wt.% in aubrites and up to 23 wt.% in enstatite chondrites and achondrites; Ca-rich sulfides are observed in all meteorite groups. Daubreélite composition does not vary among the different meteorites.

The visible-near infrared (VNIR) reflectance spectra show diagnostic features that reflect both the very low FeO content (< 0.4 wt.%) in silicates and the mineralogical and chemical variations among the samples. Aubrites present higher reflectance than enstatite chondrites and achondrites (Fig. 2). They exhibit weak mafic-related absorption bands at 0.9 µm, attributed to Fe^{2+} electronic transitions in low-Ca pyroxenes and olivine (Burns, 1993), with an additional minor absorption feature around 0.5 µm in olivine-rich portions, due to spin-forbidden Fe^{2+} transitions (Burns, 1993; Carli et al., 2018; Landi et al., 2025) (Fig. 2a). Enstatite chondrites and achondrites show nearly flat, featureless spectra with only weak or no absorptions, and in some cases a slight red slope, *i.e.* higher reflectance at longer wavelengths, related to the higher abundance of metal and sulfides (Fig. 2b). The minor absorption features occasionally observed at 1.4 and 1.9 µm are attributable to H_2O and OH of hydrated phases, indicating incipient terrestrial weathering (Burbine et al., 2002).

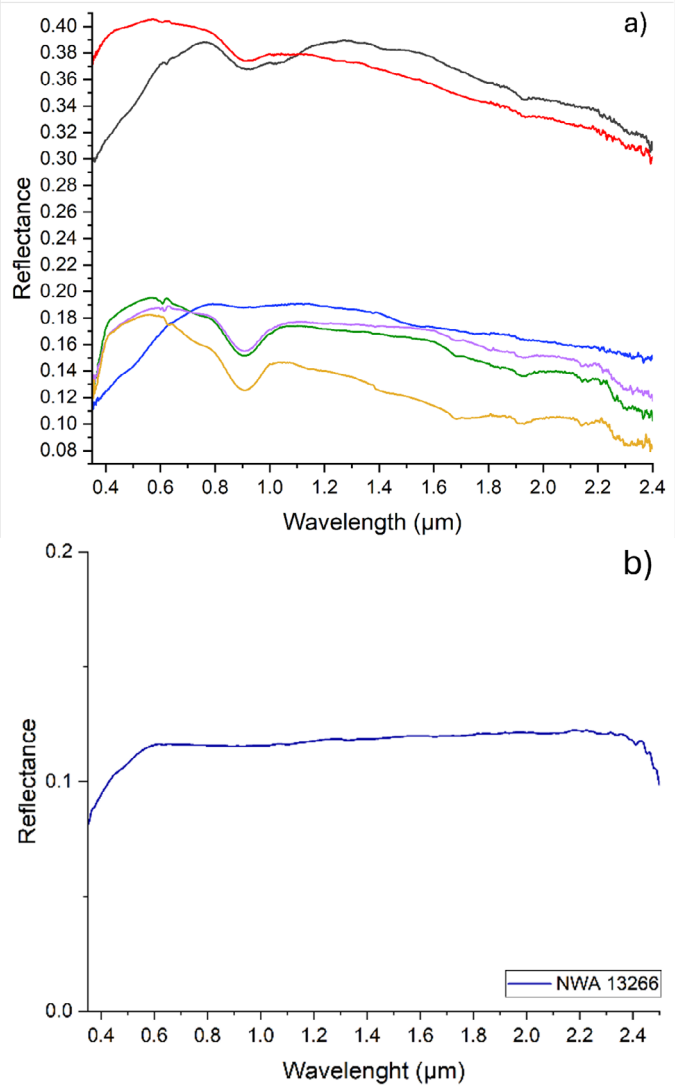

Figure 2 *Example of the VNIR reflectance spectra of the investigated samples.* ***a)*** *VNIR spectra collected in different areas of the Rantila aubrite; the absorption feature at 0.9 µm is well visible, along with a minor feature at 0.5 µm in the olivine-richer portion (blue and black spectra).* ***b)*** *Average spectrum of NWA 13266 enstatite achondrite; note the lower reflectance intensity.*

Ion irradiation on aubrites

The main spectral effects in the VNIR range are darkening, *i.e.* a decrease in the absolute reflectance value, and reddening, *i.e.*, an increase of the spectral slope (Fig. 3a). These effects are stronger with C^+ irradiation than with He^+. The IR range is less affected than the VIS range for both ions. Some differences can be observed between pellets and rocks response to irradiation: C^+ irradiation at the highest fluence ($1x10^{17}$ ions/cm^2) causes an albedo decrease in the whole spectral range for pellets but not for rocks; for rocks the darkening is much stronger with the first irradiation dose ($1x10^{16}$ ions/cm^2) for both He^+ and C^+.

Moreover, darkening is enhanced when carbon, in this case in form of organics, is pre-existing in the sample, as it has been observed in the Peña Blanca Spring spectra.

In the MIR range ion implantation produces a reduction in the spectral contrast, and shifts of the Christiansen Features (CFs), *i.e.,* reflectance minima, and Reststrahlen Bands (RBs), *i.e.,* reflectance peaks due to Si-O bonds, positions toward longer wavelengths (Fig. 3b). Shifts are in the order of hundreds of nanometres, and are bigger with He implantation. The greatest shift is observed for the main RB.

Boninites

All the investigated samples are classified as boninites, having SiO_2 > 52 wt.%, MgO > 8 wt.% and TiO_2 < 0.5 wt.% (Le Bas, 2000). The bulk compositions of samples coming from the three different localities vary slightly, as they present different mineral assemblages and aqueous alteration grade.

PAR samples are composed of olivine and clinopyroxene phenocrysts in glassy groundmass, and calcite as weathering phase. ARA samples are composed of an albitic groundmass with clinopyroxene, clinochlore and prehnite grains, minor micrometric titanite, Fe-Ti oxides, and pyrite. Olivine is not detected. The weathering in these samples is more advanced, as indicated

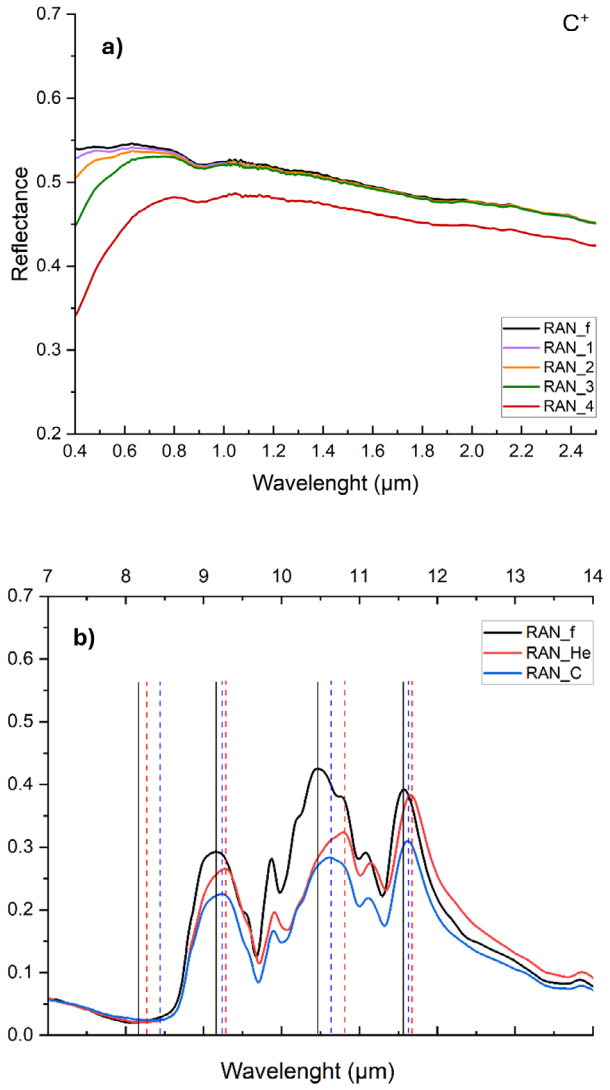

Figure 3 Ion implantation spectral effects in the VNIR range (a) and MIR range (b) for the Rantila aubrite. ***a)*** *Example for C+ implantation on pellet; f= sample before irradiation, 1= sample after the first irradiation dose, and so on.* ***b)*** *Black= sample before irradiation, red= sample after He irradiation, blue= sample after C irradiation.*

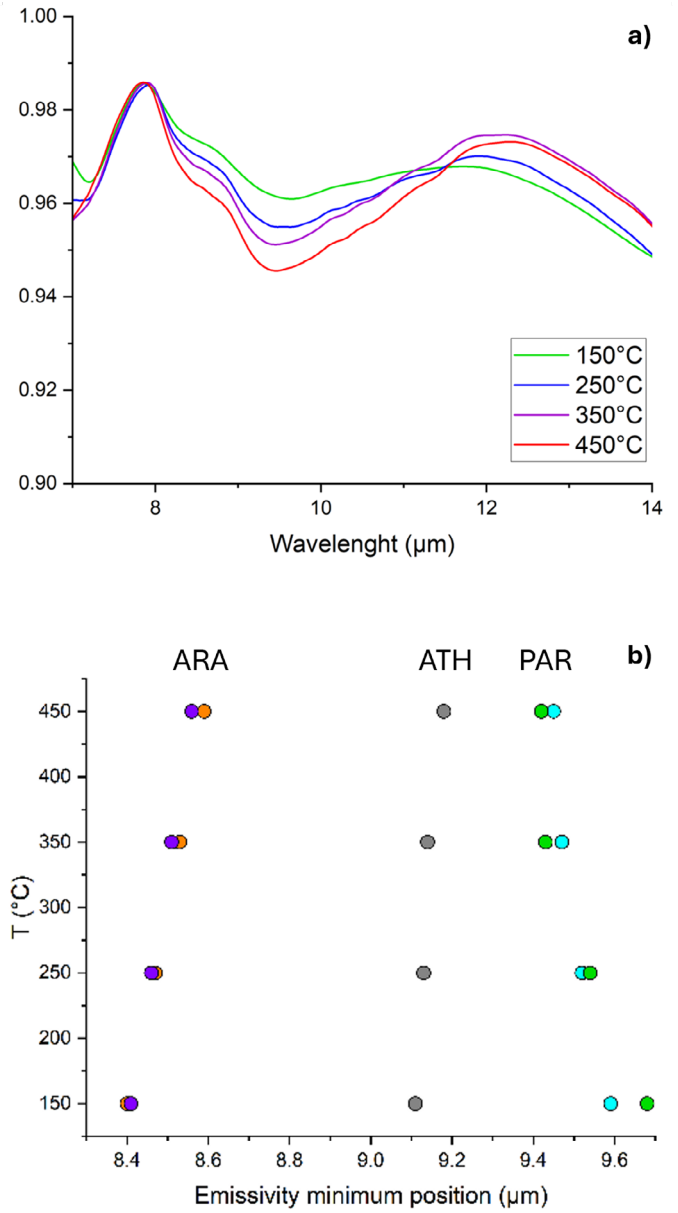

Figure 4 a) *Example of the emissivity behaviour of one of the investigated samples (PAR2) with increasing temperature.* ***b)*** *Shift of the emissivity minima positions with increasing temperature, the trend is opposite for PAR samples compared to ARA and ATH samples.*

by clinochlore replacing primary mineral grains and occupying interstitial spaces. ATH samples are holocrystalline and composed of euhedral clinopyroxene and orthopyroxene crystals surrounded by plagioclases, with minor titanite, Fe-Ti oxides and chromite. Olivine is not detected. In these samples, the weathering is more intense, and it is not uniform throughout the sample: some areas are fully altered and consist entirely of clay minerals, while others show only minor amounts of clay minerals in the interstitial spaces.

These mineralogical differences are observed in their reflectance spectra. In general, all the samples present a strong absorption band at 1 μm, related to Fe^{2+} in mafic minerals, and features at 1.4 and 1.9 μm related to hydrated phases. The band center and depth of the first and the intensity of the latter, vary among the samples coming from different localities, reflecting their mineralogical differences. The mineralogical variability is well observed in the MIR spectra, where distinct positions of the CFs are observed. CFs are located at shorter wavelengths for ARA samples, due to the higher quantity of plagioclases.

The emissivity spectra measured in the 7–14 μm, which will be investigated by MERTIS instrument, present the following changes with increasing temperature: the shifting of the CFs, *i.e.* emissivity maxima, positions; the shifting of the emissivity minima, which correspond to reflectance maxima; and the increase of the spectral contrast between CFs and RBs (Fig. 4a). Some differences can be observed in the shifting of the CFs and of the emissivity minima (Fig. 4b): the CFs shift towards shorter wavelengths for PAR (from 7.9 μm to 7.8 μm) and ATH (from 8.0 μm to 7.9 μm) samples, while the shift is towards shorter wavelengths until 350°C (7.8 μm to 7.7 μm), and then at 450°C they shift slightly back to longer wavelengths for ARA samples; the emissivity minima shift towards shorter wavelengths (from 9.6 μm to 9.4 μm) for PAR samples, and towards longer wavelengths for ARA (from 8.4 μm to 8.6 μm) and ATH samples (from 9.1 μm to 9.2 μm).

DISCUSSION

The mineralogical and chemical differences among the investigated highly reduced meteorites suggest that they may come from multiple parent bodies (Weyrauch et al., 2018). Nonetheless, their highly reduced nature led them being the best natural analogues at our disposal for Mercury's surface (Burbine et al., 2002; Udry et al., 2019; Wilbur et al., 2022). In particular, aubrites have been proposed as the best spectral natural analogues for Mercury's surface (Burbine et al., 2002) and Rantila aubrite in particular provide an interesting case study for a potential detection limit of mafic minerals from crystal field absorptions in VNIR reflectance spectroscopy (Landi et al., 2025). This meteorite contains slightly higher FeO contents in silicates (up to 0.4 wt.% compared to maximum 0.2 wt.% in other aubrites, *e.g.*, Watters & Prinz, 1979) and while the other aubrites show flat and featureless spectra with only minor mafic absorption bands (*e.g.*, Clark et al., 2004), mafic absorption bands in Rantila are stronger (Landi et al., 2025). This suggests that the potential detection limit of mafic minerals in VNIR spectra could be placed between the composition of Rantila and that of the other reduced meteorites. This is particularly relevant for Mercury's surface, as it indicates that SIMBIO-SYS instrument should be able to detect the absorption bands of exposed mafic minerals on Mercury's surface, despite their low FeO content. Comparing the VNIR spectra of these aubrites with some spectra (Vilas et al., 2016; Lucchetti et al., 2018) from the Mercury Dual Imaging System (MDIS) Camera on MESSENGER mission, it is possible to observe that the mafic absorption is located at ~ 0.9 μm and ~ 1 μm for aubrite and Mercury spectra, respectively, suggesting higher Ca-pyroxene and/or olivine amount for Mercury's surface. Also, Mercury's spectra show a ~ 0.6 μm feature associated with a higher concentration of sulfides (Vilas et al., 2016) or with a higher concentration of other transitional elements than Fe (*e.g.*, Lucchetti et al., 2018), with respect to those found in aubrites.

It is known that Mercury's surface is affected by SpWe (Domingue et al., 2014), producing chemical and physical reactions on the uppermost layers of the surface, leading to changes in the reflectance spectra. Therefore, to properly interpret the reflectance spectra from orbital observations, SpWe effect must be considered, and the ion implantation on aubrites can give us hints on the response of highly reduced surfaces to solar wind irradiations. Ion irradiation produces darkening and reddening in the VNIR range that may be caused by the amorphization of the upper layers of the irradiated surface (Brunetto et al., 2014). The mineralogy, chemical composition, and surface texture play a major role in these spectral changes (e.g., Caminiti et al., 2024). We observed that also the used ion produced different effects: C^+ ions implantation produces stronger darkening than He^+ ions. Darkening effect is slightly stronger for pellets than for rock fragments and the reddening effect induced by He^+ and C^+ is similar, while it is much stronger for pellets than for rock fragments. This could be related to the different surface roughness and scattering properties of the two surface forms suggesting also that pellets can be considered as more realistic analogue of Mercury's surface regolith, while rock fragments can represent the less SpWe affected more coherent materials. The spectral contrast reduction observed in the MIR spectral range is linked to the sample partial amorphization (Brucato et al., 2004). The observed red shifts of CFs and RBs are on the order of hundreds of nanometres, bigger than MERTIS instrument spectral resolution (90 nm, Hiesinger et al., 2020), suggesting that the instrument should be able to detect them. The shifts are similar for all the samples, and the largest shift is registered for the main RB (~ 10.5 μm), which is consistent with previous studies (e.g., Brunetto et al., 2014). He^+ irradiation induces a shift twice as large as the one produced by C^+. Therefore, the extent of the spectral changes induced by ion irradiation depends on both the nature of the ion species and the chemical and physical state of the target, revealing that surface mineralogy and texture play a key role in spectral alteration under solar wind exposure. This indicates that distinct Mercury's geochemical terranes can respond differently to SpWe (Caminiti et al., 2024).

Additionally, ion irradiation seems to induce greater effects if carbon is present in the irradiated object. These results are relevant for the study of Mercury's surface spectra, as carbon is inferred to be present on the planet's surface (1.4 ± 0.9 wt.%, Peplowski et al., 2015). Our findings support the hypothesis that carbon may be the main darkening agent explaining the planet's extremely low albedo.

The spectral differences observed between aubrites and Mercury's spectra may be linked to the fact that aubrites do not represent a perfect petrological analogue for Mercury's surface. In fact, they contain much less plagioclase and sulfides than what is inferred for Mercury's geochemical terranes (*e.g.*, Namur & Charlier, 2017; Vander Kaaden et al., 2017; Barraud et al., 2023). Enstatite chondrites, achondrites and melt rocks are not perfect petrological analogues as well, lacking olivine and clinopyroxene. Nonetheless, enstatite chondrite impact melts can help to infer how elements are distributed in the phases expected to be present on Mercury's surface and how impact processes could affect the surface, considering the same highly reducing conditions (Udry et al., 2019).

Of course, boninites are not a perfect petrological analogue for Mercury's surface, considering their different formation processes and environment, arc magmatism and hydrous conditions for terrestrial boninites (Cameron et al., 1983) and probable partial melting of a shallow portion of Mercurian mantle that did not experience hydrous and oxidizing conditions for mercurian boninites (Vander Kaaden & McCubbin, 2016), and also the extensive presence of hydrated phases from aqueous al-

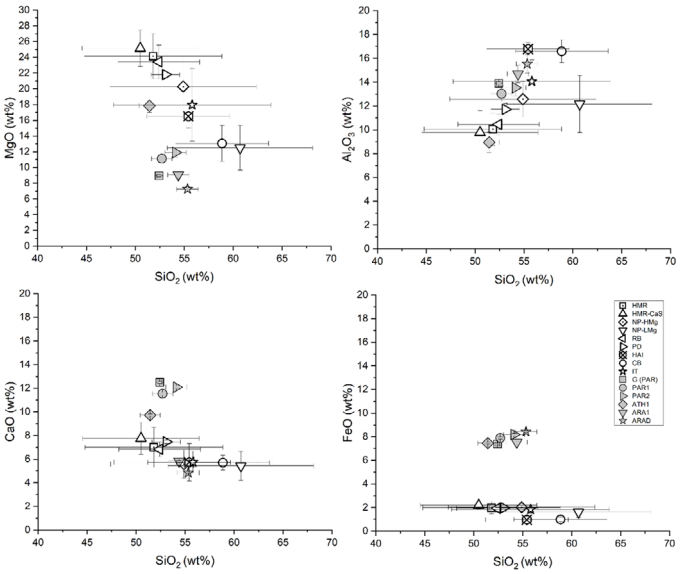

Figure 5 *Average chemical compositions of the boninite samples compared with average composition of Mercury's geochemical terranes (Vander Kaaden et al., 2017). HMR= high-Mg region; HMR-CaS= high-Mg region with high-est Ca and S; NP-HMg= northern volcanic plains with high Mg; NP-LMg= northern volcanic plains with low Mg; RB= Rachmaninoff Basin (RB); PD= pyroclastic deposits; HAI= high-Al region; CB= Caloris Basin; IT= intermediate terrane.*

teration. Nonetheless, their bulk composition presents a very good match with Mercury's terranes (Fig. 5; Landi et al., 2026). The primary compositional difference is the higher FeO content in the terrestrial samples (~ 8 wt.% compared to estimated < 2 wt.% on Mercury). This FeO content influences the reflectance spectra in the VNIR range, complicating the spectral comparison with Mercury's surface. On the other hand, MIR spectra are less affected by FeO presence, and emissivity studies on this material can be an asset to interpret the future data from MERTIS instrument. Specifically, an opposite trend is observed in the emissivity minima shifting between mafic-richer PAR samples and felsic-richer ARA and ATH samples with increasing temperature, still, the emissivity minima positions remain distinct (Fig. 4b). This suggests that mafic-richer and felsic-richer terranes should be easily identifiable with the MERTIS instrument (Ferrari et al., 2020; Landi et al., 2026).

CONCLUSIONS / FINAL REMARKS

This thesis investigates the mineralogical, chemical, and spectroscopic properties of Mercury's surface natural analogues, to contribute to the understanding of the planet's formation and evolution. The investigated analogues are highly reduced meteorites of different groups (aubrites, enstatite chondrites, achondrites, and melt rocks) and terrestrial boninites from Troodos massif, Cyprus. I focused on three main topics, investigating different aspects that can contribute to increasing our knowledge of the planet's surface: the mineralogical and spectroscopic characterization of highly reduced meteorites; laboratory simulation of space weathering on highly reduced materials (aubrites); and chemical, mineralogical and spectroscopic, including emissivity, studies on boninites.

The study of highly reduced meteorites from different groups highlights their mineralogical differences. All the investigated samples are dominated by almost FeO-free enstatite, the presence and abundance of the other mineralogical phases vary among the different samples. Aubrites show a greater heterogeneity than enstatite chondrites and achondrites. Mineral chemistry also differs among meteorites from different groups, suggesting that they originated from multiple reduced parent bodies. Although none of these meteorites represents a perfect petrological analogue of Mercury's surface, they are the best natural analogues currently available. In particular, aubrites represent the best spectral analogue, and improving our understanding of the relationship between spectral properties and mineral-chemistry of these reduced materials can provide valuable information for the future interpretation of BepiColombo data from SIMBIO-SYS and MIXS instruments.

For a consistent comparison between aubrites and Mercury's surface spectra, the effect of SpWe on the planet's surface must be taken into account. Therefore, ion irradiation experiments were conducted on aubrites to simulate the effects of solar wind irradiation on the spectra of highly reduced materials. The observed spectral changes include darkening and reddening in the VNIR range, as well as red shifts of the CFs and RBs positions, and a reduction of spectral contrast in the MIR range. The extent of these changes depends on the composition of the target materials, on their surface form (with differences observed between pellets and rock fragments), and on the type of ion used. The spectral changes induced by ion irradiation likely result from amorphization of the upper layers. Based on our observations, the presence of carbon in the target material might cause enhanced spectral changes, especially darkening, which is particularly interesting for Mercury, where carbon is present on the surface. We can also assume that the different Mercury's geochemical terranes might react differently to SpWe, depending on their composition.

Additional spectral information that can be useful for understanding Mercury's surface was obtained from the investigation of boninites. These terrestrial samples show mineral assemblages that do not exactly match the inferred mineralogy of Mercury's surface (e.g., the presence of hydrated phases from aqueous alteration and the absence of metals and Mg, Ca, Mn sulfides). On the other hand, bulk composition analyses confirmed a good match in major element contents (wt.%) with the estimated composition of Mercury's geochemical terranes, although FeO is substantially higher in the terrestrial rocks. Nonetheless, the study of emissivity behaviour in the MIR range is relevant for Mercury. In particular, the emissivity minima shift in opposite directions for mafic-richer and felsic-richer samples. However, the minima positions remain distinct, suggesting that MERTIS will easily identify mafic-richer and felsic-richer terranes.

Overall, the results presented in this thesis can support the interpretation of Mercury's surface data. By relating the mineralogy and chemical composition to spectral behaviour, and considering the effects of SpWe and extreme temperature variations, this work provides information that could be useful for the BepiColombo mission. Specifically, it can help in the understanding and linking of the data from SIMBIO-SYS, MERTIS, and MIXS instruments. Linking the information coming from these three instruments, along with the others onboard the mission, will give us insights into Mercury's formation and evolution.

REFERENCES

Barraud, O., Besse, S., Doressoundiram, A. (2023) - Low sulfide concentration in Mercury's smooth plains inhibits hollows. Sci. Adv., 9, eadd6452.

Brucato, J.R., Strazzulla, G., Baratta, G., Colangeli, L. (2004) - Forsterite amorphisation by ion irradiation: Monitoring by infrared spectroscopy. Astron. Astrophys., 413(2), 395-401.

Brunetto, R., Lantz, C., Ledu, D., Baklouti, D., Barucci, M.A., Beck, P., Delauche, L., Dionnet, Z., Dumas, P., Duprat, J., Engrand, C., Jamme, F., Oudayer, P., Quirico, E., Sandt, C., Dartois, E. (2014). Ion irradiation of Allende meteorite probed by visible, IR, and Raman spectroscopies. Icarus, 237, 278–292.

Burbine, T.H., McCoy, T.J., Nittler, L., Benedix, G.K., Cloutis, E.A., Dickinson, T.L. (2002) - Spectra of extremely reduced assemblages: Implications for Mercury. Meteorit. Planet. Sci., 37,1233-1244.

Burns, R.G. (1993) - Mineralogical Applications of Crystal Field Theory. 2nd Edition, Cambridge University Press, Cambridge.

Cameron, W.E., McCulloch, M.T., Walker, D.A. (1983) - Boninite petrogenesis: chemical and Nd-Sr isotopic constraints. Earth Planet. Sci. Lett., 65, 75-89.

Caminiti, E., Lantz, C., Besse, S., Brunetto, R., Carli, C., Serrano, L., Mari, N., Vincendon, M., Doressoundiram, A. (2024) - Effects of ion irradiation on Mercury terrestrial analogues in the visible to mid-infrared. Icarus, 420, 116191.

Carli, C., Pratesi, G., Moggi-Cecchi, V., Zambon, F., Capaccioni, F., Santoro, S. (2018) - Northwest Africa 6232: Visible–near infrared reflectance spectra variability of an olivine diogenite. Meteorit. Planet. Sci., 53(10), 2228–2242.

Chauvin, N., Dayras, F., Le Du, D., Meunier, R. (2004) - SIDONIE: an electromagnetic isotope separator for preparation of high purity thin targets. Nucl. Instrum. Methods Phys. Res. A, 521, 149–155.

Clark, B.E., Bus, S.J., Rivkin, A.S., McConnochie, T., Sanders, J., Shah, S., Hiroi, T., Shepard, M. (2004) - E-type asteroid spectroscopy and compositional modeling, J. Geophys. Res., 109, E02001.

Cremonese, G., Capaccioni, F., Capria, M.T., Doressoundiram, A., Palumbo, P., Vincendon, M., et al. (2020) - SIMBIO-SYS: Scientific Cameras and Spectrometer for the BepiColombo Mission. Space Sci. Rev., 216(75).

Domingue, D.L., Chapman, C.R., Killen, R.M., Zurbuchen, T.H., Gilbert, J.A., Sarantos, M., et al. (2014) - Mercury's weather-beaten surface: understanding mercury in the context of lunar and Asteroidal space weathering studies. Space Sci. Rev., 181, 121–214.

Ferrari, S., Nestola, F., Massironi, M., Maturilli, A., Helbert, J., Alvaro, M., Domeneghetti, M.C., Zorzi, F. (2014) - In-situ high-temperature emissivity spectra and thermal expansion of C2/c pyroxenes: Implications for the surface of Mercury. Am. Mineral., 99, 786–792.

Ferrari, S., Maturilli, A., Carli, C., D'Amore, M., Helbert, J., Nestola, F., Hiesinger, H. (2020) - Thermal infrared emissivity of felsic-rich to mafic-rich analogues of hot planetary regoliths. Earth Planet. Sci. Lett., 534, 116089.

Fraser, G.W., Carpenter, J.D., Rothery, D.A., Pearson, J.F., Martindale, A., Huovelin, J., et al. (2010) - The Mercury Imaging X-ray Spectrometer (MIXS) on BepiColombo. Planet. Space Sci., 58, 79–95.

Hiesinger, H., Helbert, J., Alemanno, G., Bauch, K.E., D'Amore, M., Maturilli, A., et al. (2020) - Studying the Composition and Mineralogy of the Hermean Surface with the Mercury Radiometer and Thermal Infrared Spectrometer (MERTIS) for the BepiColombo Mission: An Update. Space Sci. Rev., 216(110).

Keil, K. (2010) - Enstatite achondrite meteorites (aubrites) and the history of their asteroidal parent bodies. Chem. Erde, 70, 295-317.

Landi, A.I., Gaft, M., Carli, C., Capaccioni, F., Pratesi, G. (2025) - Insights into the mineralogy of the Rantila aubrite: A luminescence and VNIR reflectance spectroscopy study. Icarus, 441, 116725.

Landi, A.I., Carli, C., Maturilli, A., Alemanno, G., Barraud, O., Capaccioni, F., Pratesi, G. (2026) - From Earth to Mercury: Compositional, reflectance spectroscopy, and emissivity studies on boninites as surface natural analogs. J. Geophys. Res. Planets, 131, e2025JE009382.

Le Bas, M.J. (2000). IUGS Reclassification of the High-Mg and Picritic Volcanic Rocks. J. Petrol., 41(10), 1467-1470.

Lucchetti, A., Pajola, M., Galluzzi, V., Giacomini, L., Carli, C., Cremonese, G., et al. (2018) - Mercury Hollows as Remnants of Original Bedrock Materials and Devolatilization Processes: A Spectral Clustering and Geomorphological Analysis. J. Geophys. Res. Planets, 123, 2365–2379.

Maturilli, A., Helbert, J., St. John, J.M., Head, J.W., Vaughan, W.M., D'Amore, M., Gottschalk, M., Ferrari, S. (2014) - Komatiites as Mercury surface analogues: spectral measurements at PEL. Earth Planet. Sci. Lett., 398, 58–65.

Maturilli, A., Helbert, J., Varatharajan, I., D'Amore, M. (2017) - Emissivity Spectra of Mercury Analogues under Mercury Pressure and Temperature Con-

ditions. EPSC Abstracts, Vol. 11, EPSC2017-610, 2017.

Namur, O. & Charlier, B. (2017) - Silicate mineralogy at the surface of Mercury. Nat. Geosci.,10, 9–13.

Nittler, L.R. & Weider, S.Z. (2019) - The surface composition of Mercury. Elements, 15, 33-38.

Peplowski, P.N., Lawrence, D.J., Evans, L.G., Klima, R.L., Blewett, D.T., Goldsten, J.O., et al. (2015) - Constraints on the abundance of carbon in near-surface materials on Mercury: results from the MESSENGER gamma-ray spectrometer. Planet. Space Sci., 108, 98–107

Rothery, D.A., Massironi, M., Alemanno, G., Barraud, O., Besse, S., Bott, N. et al., (2020) - Rationale for BepiColombo Studies of Mercury's Surface and Composition. Space Sci. Rev., 216(66).

Solomon, S.C., Nittler, L.R., Anderson, B.J. (2018) - MERCURY: The View after MESSENGER. Cambridge University Press.

Udry, A., Wilbur, Z.E., Rahib, R.R., McCubbin, F.M., Vander Kaaden, K.E., McCoy, T.J. et al. (2019) - Reclassification of four aubrites as enstatite chondrite impact melts: Potential geochemical analogs for Mercury. Meteorit. Planet. Sci., 54(4), 785-810.

Vander Kaaden, K.E. & McCubbin, F.M. (2016) - The origin of boninites on Mercury: an experimental study of the northern volcanic plains lavas. Geochim. Cosmochim. Acta, 173, 246–263.

Vander Kaaden, K.E., McCubbin, F.M., Nittler, L.R., Peplowski, P.N., Weider, S.Z., Frank, E.A., McCoy, T.J. (2017) - Geochemistry, mineralogy, and petrology of boninitic and komatiitic rocks on the mercurian surface: in-sights into the mercurian mantle. Icarus, 285, 155–168.

Vilas, F., Domingue, D.L., Helbert, J., D'Amore, M., Maturilli, A., Klima, R.L. et al. (2016) - Mineralogical indicators of Mercury's hollows composition in MESSENGER color observations. Geophys. Res. Lett., 43(4), 1450-1456.

Watters, T.R. & Prinz, M. (1979) - Aubrites: Their origin and relationship to enstatite chondrites. Proc. Lunar Planet. Sci. Conf. 10th,1073-1093.

Weider, S.Z., Nittler, L.R., Starr, R.D., Crapster-Pregont, E.J., Peplowski, P.N., Denevi, B.W., et al. (2015) - Evidence for geochemical terranes on Mercury: Global mapping of major elements with MESSENGER's X-Ray Spectrometer. Earth Planet. Sci. Lett., 416, 109–120.

Weyrauch, M., Horstmann, M., Bischoff, A., (2018) - Chemical variations of sulfides and metal in enstatite chondrites—Introduction of a new classification scheme. Meteorit. Planet. Sci., 53(3), 394–415.

Wilbur, Z.E., Udry, A., McCubbin, F.M., Vander Kaaden, K.E., DeFelice, C., Ziegler, K., et al. (2022) - The effects of highly reduced magmatism revealed through aubrites. Meteorit. Planet. Sci., 57(7), 1387-1420.